CrossMark

Study of microstructure and magneto-transport properties in $Bi_{1.6}Pb_{0.4}Sr_2Ca_3Gd_xCu_4O_\delta$ superconducting systems

H. Ağıl[1]

Abstract

The role of Gd addition in the $Bi_{1.6}Pb_{0.4}Sr_2Ca_3Gd_xCu_4O_y$ (x = 0.0, 0.1, 0.2, 0.3 and 0.4) system was examined by X-ray powder diffraction, scanning electron microscopy, critical current density (J_c) and magneto-transport measurements. The samples were fabricated by the conventional solid state reaction method. The analysis showed that the critical temperature (T_c) and hole number (p) of the materials decreased while the room temperature resistances increased with the addition of Gd. The resistance–temperature dependence for the low-resistance regions of the transition can be determined by the thermally activated flux flow model. The upper critical field [$H_{c2}(T)$] values calculated by using this model decreased with the addition of Gd. Furthermore, it was observed that the activation energy (U_0) decreased both with the increase in the amount of Gd and applied magnetic field. The degradation of the superconducting properties of the samples may be related to the alteration of the structural, electronic and magnetic properties of the materials depending on the presence of the Gd ions. As a result, the decrease in the number of holes and the magnetic properties of Gd ions are thought to be the fundamental reasons for the deterioration of the superconducting properties of the materials. It has been observed that Gd additions from the microstructure studies of the materials affected the surface morphology negatively.

1 Introduction

Many research groups around the world have been working extensively on high-temperature superconductors, discovered in 1987 and 1988 (especially YBCO ($T_c = 93$ K) [1] and BSCCO ($T_c = 110$ K) [2]), so that they can be used in practice.

$(Bi,Pb)_2Sr_2Ca_2Cu_3O_{10+\delta}$ (Bi-2223) phase appears to be one of the technologically most important high T_c phases in the Bi–Sr–Ca–Cu–O system, although it is difficult to prepare in pure form. It has been observed that partial displacement of bismuth (Bi) and lead (Pb) improves the preparation of almost single phase 2223 sample and causes an increase in T_c [3–5]. The partial substitution of Bi with Pb takes place in the general formula $Bi_{2-x}Pb_xSr_2Ca_2Cu_3O_\delta$ where the optimum amount of Pb (x) is between 0.3 and 0.4 [6–8]. It has been reported that bismuth substitution with lead leads to more stable material formation and high-T_c phase formation [9]. The Ca_2PbO_4 phase formed during the heat treatment

process also plays an important role in the formation of the high-T_c phase [10–13]. Various production techniques have been reported to improve the Bi-based superconductors [14–20].

The Bi-2223 phase requires an initial powder with a high density [21]. Unfortunately, this density easily dissipates during the heat treatment. The heat treatment of Bi-2223 is a long-term process that must be applied carefully. Otherwise, the sample can be separated into Bi-2212 phase, which is the second phase [2].

One of the methods used to improve the critical parameters (T_c, J_c, H_c, etc.) of superconducting samples is to make doping or adding [22–24]. The effects on the superconducting properties of rare earth element addition to the BSCCO superconductor have been a major concern for technological applications. The reason for this is that the doping is an effective method for improving the structural, transport, superconducting and flux pinning properties that allow Bi-based superconductors to be suitable for application at higher temperatures and magnetic fields. Rare earth elements have an incomplete inner shell, different magnetic moments and different ionic radii. For this reason, they are of great importance as an additive material for studying the physical properties of high temperature superconductors. Numerous

✉ H. Ağıl
hasanagil@hakkari.edu.tr

1 Department of Material Science and Engineering, Faculty of Engineering, Hakkari University, 30000 Hakkari, Turkey

reports on the effect of different elements of lanthanides series (La, Ce, Pr, Nd, Sm, Eu, Dy, Ho…) on the Ca or Sr site of the Bi-2223 phase are presented. The use of rare earth elements instead of Ca in Bi-2223 system is very interesting. Because, these additions lead to structural stability and help to understand the structure and diversity of charge carriers. Although many of the previous studies have developed the structural stability of Bi-2223 systems of cation substitute, superconducting properties such as T_c have been shown to suppress as the amount of addition increases. In this work, the effects of critical parameters on the Bi-2223 phase were investigated by adding Gd. Gadolinium has been reported to improve the lateral levitation force due to its magnetic properties [25]. For this reason, structural and magneto transport effects of Gd addition to BSCCO superconductor were investigated. The samples were characterized by X-ray diffraction, scanning electron microscopy, critical current density and magneto resistance measurements.

2 Experimental procedure

The pristine ($Bi_{1.6}Pb_{0.4}Sr_2Ca_3Cu_4O_\delta$) and Gd-added ($Bi_{1.6}Pb_{0.4}Sr_2Gd_xCa_3Cu_4O_\delta$, x = 0.1, 0.2, 0.3 and 0.4) samples were prepared by the conventional solid state reaction method. As the samples were prepared, high purity bismuth oxide (Bi_2O_3), lead oxide (PbO), strontium oxide (SrO), calcium oxide (CaO), gadolinium oxide (Gd_2O_3) and copper oxide (CuO) were used as starting powder. First, the starting powders were weighed accurately according to the stoichiometric ratio. Then, the powders were homogenously mixed and ground using an agate mortar and pestle for 30 min. After grinding, the powders were calcined for 12 h in air at 700 and 800 °C, respectively. Between each calcination process, the powders were subjected to intermediate grinding for 30 min. The resulting powder was then pressed into the pellet. Finally, the pellets were sintered for 120 h at 845 °C in air. Samples prepared with different Gd addition with x = 0, 0.1, 0.2, 0.3 and 0.4 in $Bi_{1.6}Pb_{0.4}Sr_2Gd_xCa_3Cu_4O_\delta$ will be denoted as Gd00, Gd01, Gd02, Gd03 and Gd04, respectively.

Phase analysis of all the samples was performed with X-ray powder diffraction (Bruker D8 Advance XRD instrument). The lattice parameters of the fabricated samples were determined with PDF Diffrac Plus 2000 and Whatfor analysis program. The size, shape and microstructure of the particles were observed through the images of the samples taken by scanning electron microscopy (JEOL JSM 7600F). The critical temperature (T_c) was found from the DC magnetization measurements (M–T) of the samples. In addition, the critical current density (J_c) was theoretically calculated by using Bean critical state model from the width of M–H curves [26]. The electrical resistivity of the samples is measured by the standard four-probe technique in closed cycle
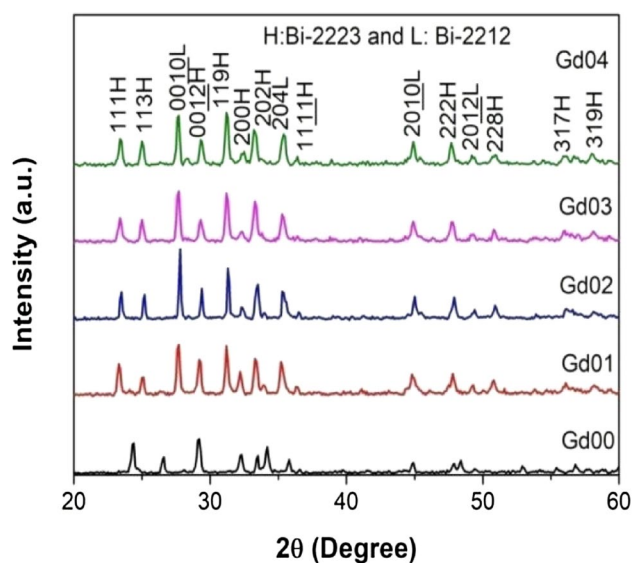

Fig. 1 X-ray diffraction pattern of all the samples

Table 1 Lattice parameters of all samples

Sample	a (Å)	b (Å)	c (Å)
Gd00	5.428	5.453	36.989
Gd01	5.447	5.443	36.687
Gd02	5.446	5.443	36.566
Gd03	5.465	5.469	36.609
Gd04	5.470	5.456	36.547

refrigerator within the range of (10–300 K). In addition, the upper critical field (H_{c2}) and irreversibility field (H_{irr}) were also determined by the magneto resistance measurements.

3 Results and discussion

X-ray diffraction data were taken with Cu-Kα radiation at 2θ = 20°–60° with a scan speed of 3°/min and a step increase of 0.02° at room temperature. The XRD patterns of all samples are shown in Fig. 1. From the XRD analysis it is seen that the main phase is Bi-2223 in all samples and that some of these peaks belong to the phase Bi-2212. It was observed that the intensity of the peaks corresponding to the Bi-2223 phase increased until x ≥ 0.3 and decreased after this value. Assuming that the phases Bi-2223 and Bi-2212 have orthorhombic symmetry, the lattice parameters *a, b* and *c* were calculated using the *d* values and (*hkl*) parameters and are shown in Table 1. These calculations were performed with the help of the Whatfor analysis program and data from XRD measurements. A uniform distribution in the lattice parameters was not observed with increasing amount of Gd. Compared to the ionic radius of Gd^{3+} (0.97 Å) with

Bi^{3+} (0.96 Å), Sr^{2+} (1.12 Å) and Ca^{2+} (0.99 Å), Gd ions can replace any of these elements. Nevertheless, substitution of Gd^{3+} for Bi^{3+} does not significantly change the superconducting properties.

The surface morphology of the pristine and added samples was examined by SEM. Figure 2 shows surface images for all samples. The microstructure of the pure sample is significantly different from the additive samples. With increasing Gd addition, the grain connectivity of the materials appears to be getting worse. As the grains are better oriented, the surface of the pure sample is smoother. The greater the amount of Gd-added samples are, the smaller the grain size is. SEM images of Gd00 and Gd01 exhibit better crystallization compared to other samples, and Gd00 is the best. Within these five samples, the worst surface morphology belongs to the Gd04 sample. It is thought that the reason for this is caused by the voids in the material, and the melts in the process of heat treatment. Scanning electron microscopy results indicate that the microstructure of the materials is degraded by Gd addition.

Critical temperatures of all samples (T_c) were determined by both dc resistance and magnetization measurements. First, we focused on the results obtained from the magnetization (M–T) measurements. Figure 3 shows the magnetization curves of all samples as a function of the temperature.

All materials exhibit diamagnetic behaviors, which is characteristic of superconductors. As the amount of Gd increases,
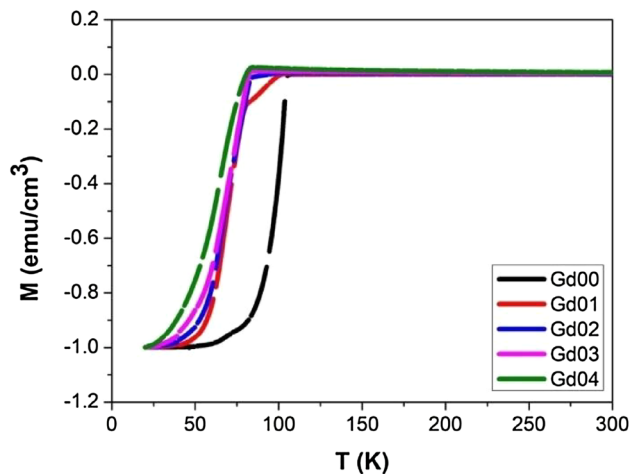
Fig. 3 Magnetization versus temperature M(T) for all the samples
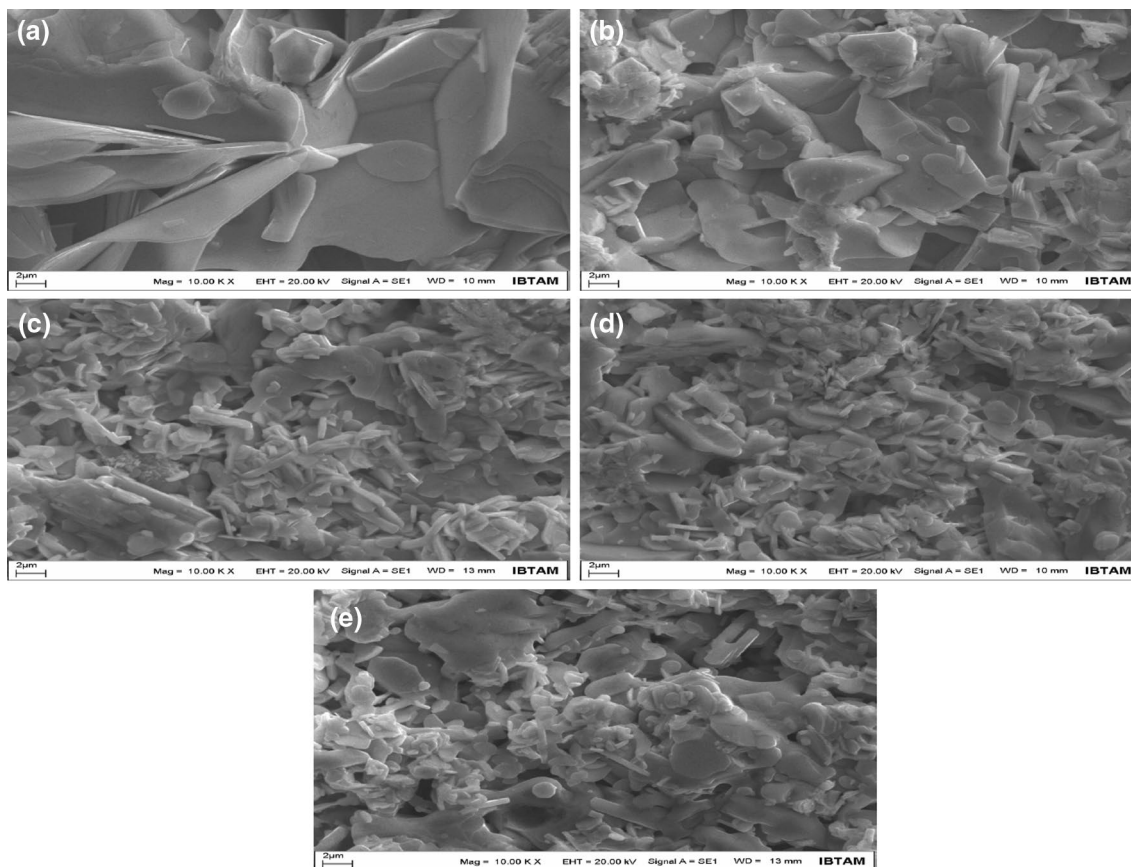
Fig. 2 Scanning electron micrographs of **a** Gd00, **b** Gd01, **c** Gd02, **d** Gd03 and **e** Gd04

the transition temperatures decrease. Depending on the amount of Gd in the materials, the transition temperatures range from 80 to 105 K. These values indicate that there is a high-T_c phase in the samples as well as a low-T_c phase. The critical transition temperatures (T_c) obtained from the magnetization curves of the samples are given in Table 1.

The variation of the critical temperature (T_c) with the amount of Gd (x) is shown in Fig. 4. It has been observed that critical temperature values have decreased while x increased. This reduction is thought to be related to the Bi-2212 phase exists in the samples.

Considering the magnetization behavior of the materials, Bi-2212 phase appears to influence the properties of Bi-2223 phase. This is one of the reasons for the reduction of the critical temperature of the materials.

In low temperature superconductors, the T_c increases monotonically with an increase in the number of charge carriers [$T_c(p) \propto p$]. On the other hand, in cuprate superconductors, this dependence is not monotonic. It is known that there is a parabolic relationship between the critical temperature and the number of holes. Number of holes is calculated using the following equation [27].

$$\frac{T_c}{T_c^{\max}} = 1 - 82.6 \, (p - 0.16)^2 \tag{1}$$

In this equation, T_c^{max} is the maximum critical temperature for a given compound. For high temperature superconductors, superconductivity occurs when p value is between 0.05 and 0.27. The number of holes (p) are calculated via the following relation:

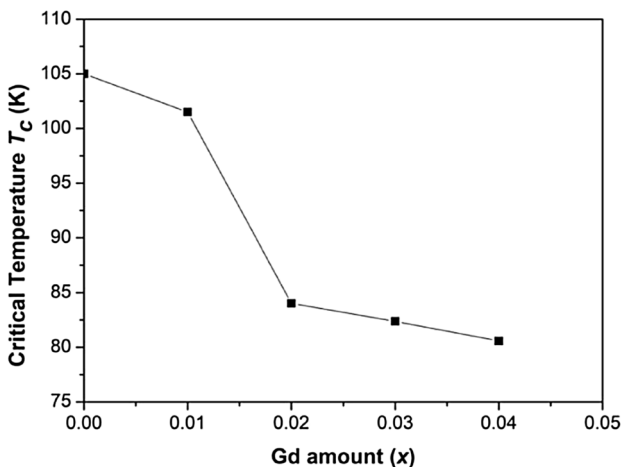$$p = 0.16 - \left[\frac{\left(1 - \frac{T_c}{T_c^{\max}}\right)}{82.6} \right]^{1/2} \tag{2}$$

where T_c^{max} is taken as 110 K for the (Bi, Pb)-2223 system [27]. The p values for pure Bi-2223 have been reported to vary from 0.116 to 0.160 [28]. In Fig. 5, the relationship between T_c and p appears to be almost parabolic. The T_c of high-T_c superconducting materials varies depending on the hole concentration of CuO_2 plane. Therefore, the critical temperature of added materials decreases with decreasing hole concentration.

The number of holes decreased from 0.136 to 0.103 due to the increase in Gd and the decrease in T_c. This is thought to be due to the deterioration of the intergranular connectivity of the samples. Figure 6 shows that the number of holes decreases with increasing Gd addition. It is seen that the number of holes of pure material is larger when compared with the additive materials. This is a consequence of the degradation of the superconducting parameters of the materials.
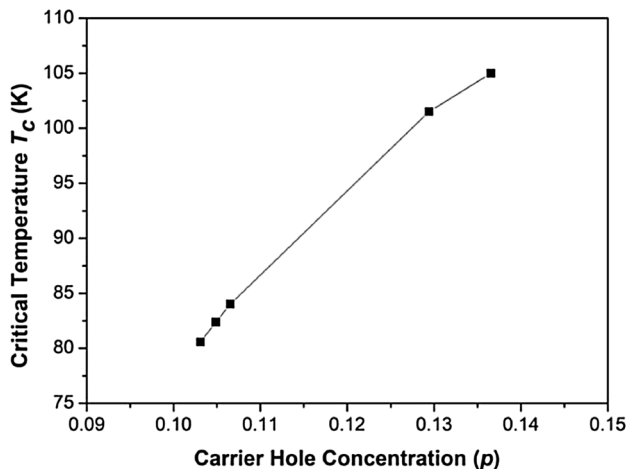
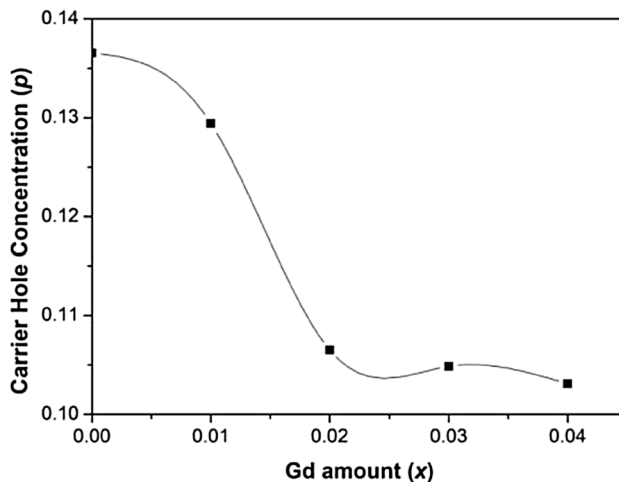**Fig. 5** Superconducting transition temperature versus hole concentration

Fig. 4 The variation of critical temperature with Gd amount

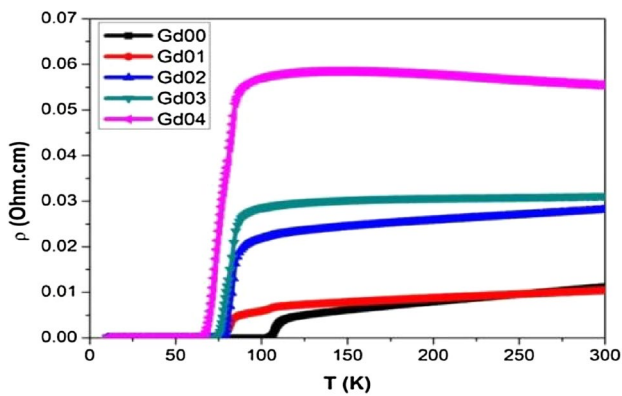**Fig. 6** Carrier hole concentration versus Gd amount of the samples

Fig. 7 Temperature dependence of resistivities in all samples

Table 2 The T_c^{zero} (K) of the samples under several magnetic fields

Samples	0 T	1 T	3 T	5 T
Gd00	105	72	60	56
Gd01	75	48	39	35
Gd02	74	45	36	32
Gd03	72	37	29	27
Gd04	67	30	24	22

To determine the critical temperature (T_c), resistivity measurements were also performed as a function of the temperature in the range of 10–300 K. Figure 7 shows the resistivity measurements of all samples as a function of temperature. The critical temperature (T_c) values are shown in Table 2. The T_c value of pure sample was 105 K, while this value of Gd04 decreased to 67 K. Simon et al. [29] and Kishore et al. [30] similarly reported a decrease in the critical temperature of our results. It was also found that the room temperature resistivity value increased from 11.23 mΩ cm for Gd00 to 55.45 mΩ cm for Gd04. In this study, it is thought that some of the added Gd is located at grain boundaries, as shown by an increase in room temperature resistivity, while the rest may be replaced by calcium or strontium site in the $Bi_{1.6}Pb_{0.4}Sr_2Ca_3Cu_4O_\delta$ system [31].

The upper critical field (H_{c2}), the irreversibility field (H_{irr}) and the activation energies (U_0) of the samples were determined from resistivity–temperature (ρ–T) curves under magnetic fields up to 5 T. Magnetoresistance measurements were carried out at 0, 1, 3 and 5 T. The magnetic field was applied perpendicular to the current flow direction. The H_{c2}(T) and H_{irr}(T) are defined as the fields in the temperature-dependent resistance under constant magnetic field and are expressed by the following equations [32, 33]:

$$R\left(H_{c2}, T\right) = 0.9R_n \tag{3}$$

$$R\left(H_{irr}, T\right) = 0.1R_n \tag{4}$$

In these equations, R_n is defined as the normal state resistance at 110 K. Figure 8 shows the temperature dependence of normalized resistance under the applied magnetic fields for all materials. The resistances of all materials were normalized at 120 K. T_c^{zero} of all materials under several applied magnetic field values are given in Table 2. In non-magnetic field measurements, the T_c^{zero} values of the samples decreased with an increase in Gd amount. Due to the addition of Gd, it is considered that there is a direct correlation between the decrease in the transition temperature and the decrease in the number of holes [34].

The T_c value of the Bi-2223 phase relies on the density of the mobile charge carriers in the CuO_2 plane and the average Cu value consequently [35]. The displacement of Ca^{2+} ions with Gd^{3+} ions is associated with a decrease in Cu valence [36, 37]. As a consequence, it is anticipated that T_c decreases with increasing amount of Gd. Compared with pure material, it has been observed that the transition in the doped materials is widening. This implies that both impurities and weak bonds exist between the superconducting particles.

In magnetoresistance measurements, as the magnetic field increases, the T_c^{offset} values of all samples decrease monotonically. As the applied magnetic field increases, the expansion of the transition is seen to increase even more. In magnetic measurements, the bond between the particles of the materials is sensitive to the applied magnetic field. The resistivity measurements in the applied magnetic fields show that the T_c^{onset} values do not shift considerably with the magnetic field [38]. However, T_c^{offset} values are dramatically reduced with the applied magnetic field. The basic mechanism of loss in the magnetic field is due to the motion of the flux lines [39].

The activation energy was calculated based on the applied magnetic field and Gd addition. To do this, resistive transition data are used under applied magnetic fields. To determine the magnetic field dependence of the activation energy, resistance–temperature measurements were performed under different magnetic fields. At temperatures below T_c, TAFF is a significant loss mechanism that occurs during the resistive transition [40–43].

Transport measurements can be made to obtain more sensitive values of the activation energy. Because one of the parameters affecting the value of activation energy in magnetic measurements is the expansion of the transition [34, 44]. Activation energies are calculated using linear fitting of the low-resistance region of the transition [40, 45]. The activation energy (U_0) is found by the slope of the linear part of the low-resistance region in the ln ρ–1/T graph. These graphs are shown in Fig. 9 for all samples. The resistivity ρ is supposed to have the following equation:

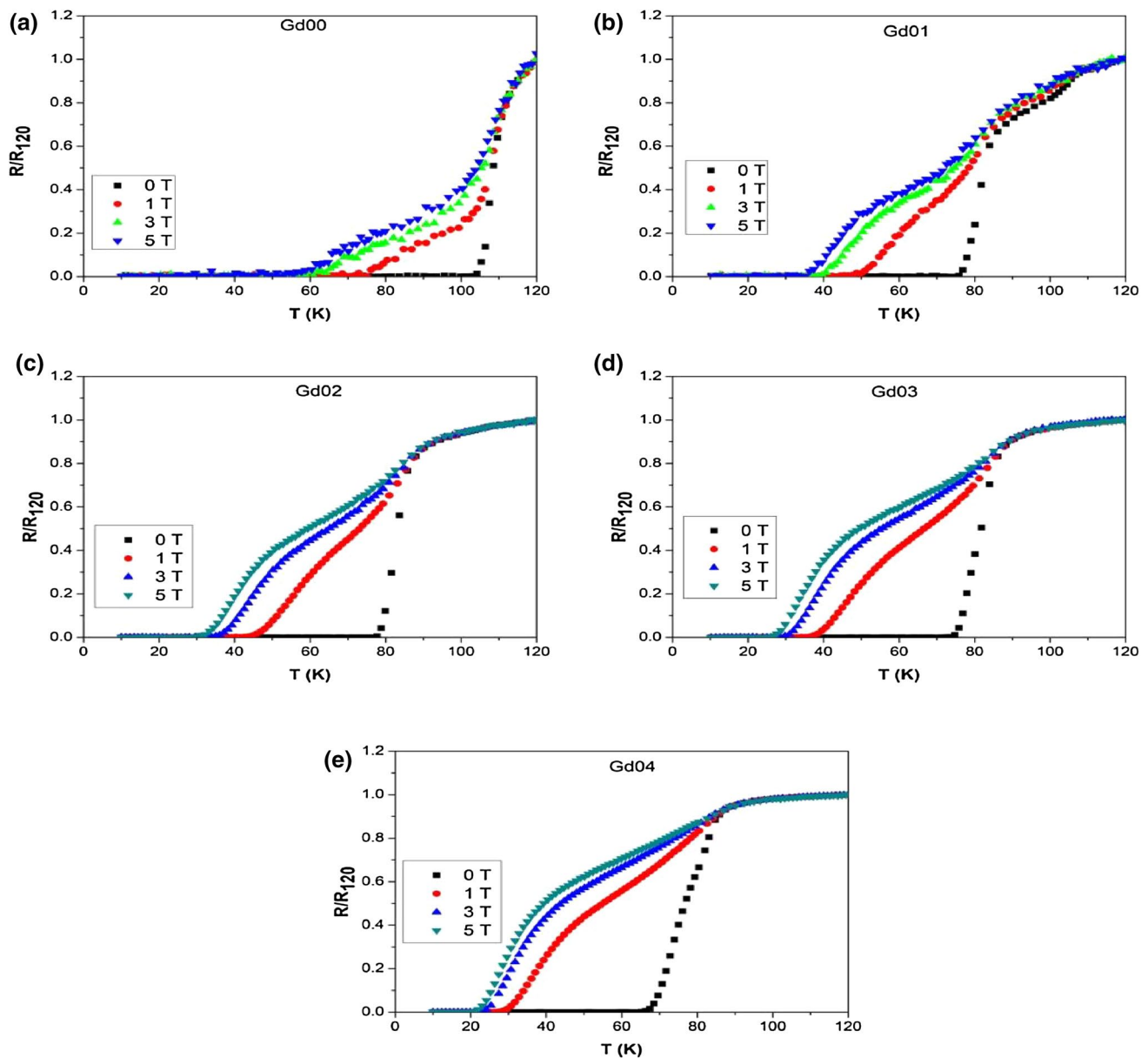$$\rho(T) = \rho_0 \exp\left(-\frac{U_0}{k_B T}\right) \tag{5}$$

Fig. 8 **a–e** Temperature dependence of normalized resistance for all samples at various magnetic fields

In this equation, ρ_0 is the pre-exponential factor, U_0 is the activation energy and k_B is the Boltzmann constant. The U_0 values which are calculated using this equation are given in Table 3. When the values in the table are examined, it is seen that the activation energy is decreased by the increase of the Gd addition and the applied magnetic field. Similar results have also been reported in [46, 47].

In order to examine the field dependence of the activation energy, a log–log graph of the activation energy against the applied magnetic field is plotted in Fig. 10. The relationship between the activation energy and the magnetic field is linear, as is clear from the diagram.

The behavior of the calculated H_{c2} and H_{irr} against the temperature is given in Fig. 11. The H_{c2} and H_{irr} values were recorded at lower temperatures with an increase in the amount of Gd. This result implies that the superconducting properties of the materials deteriorate with Gd addition. From the point of view of the irreversibility field, it appears that the pure sample has better properties. This behavior of the irreversibility field with Gd addition shows that it deteriorates the pinning properties of the materials. This situation is also in agreement with the activation energy data.

The field dependence of the calculated critical current densities (J_c) using the Bean critical state model [26]
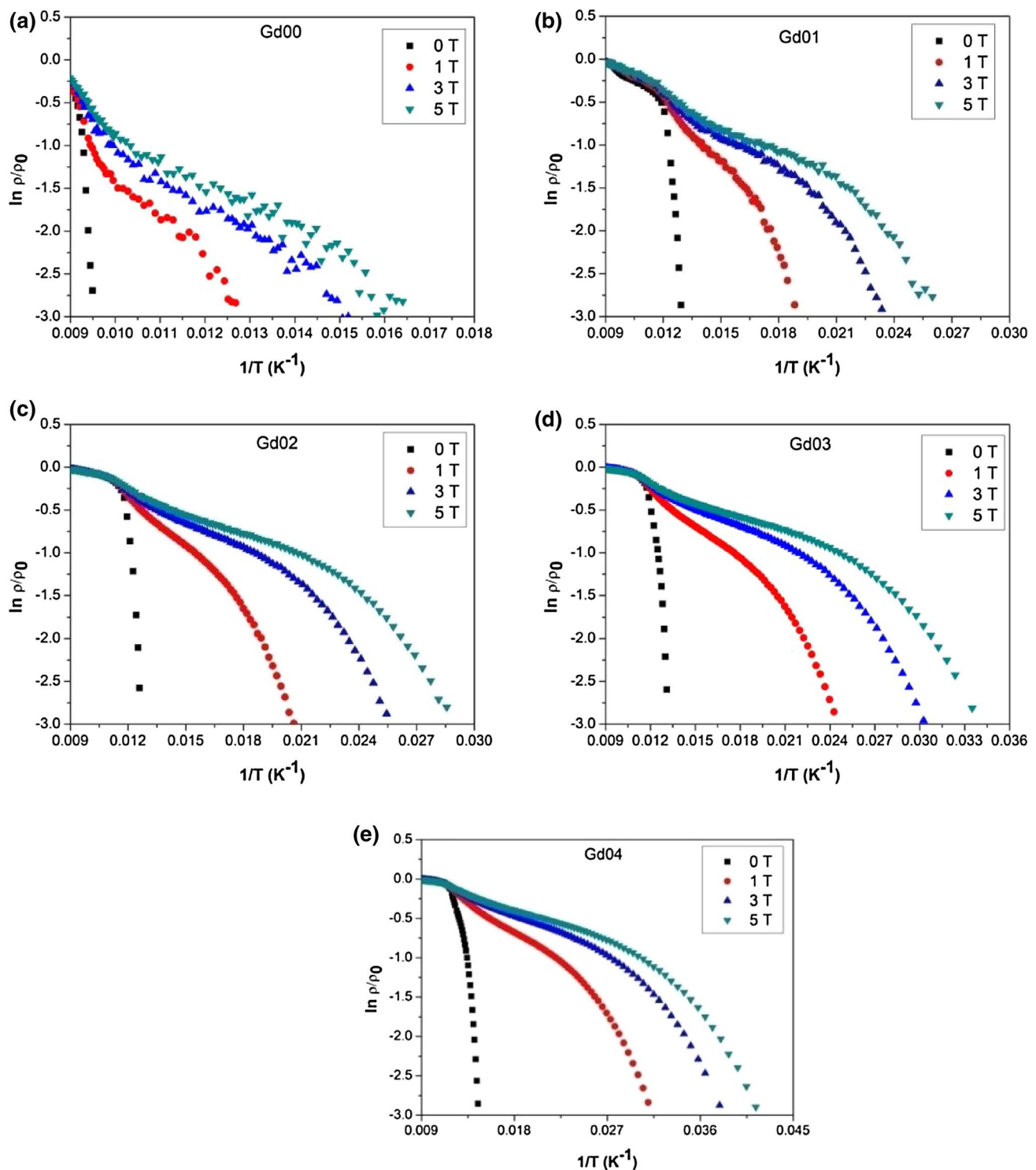
Fig. 9 ln ρ–1/T curves of all samples

from the width of M–H curves is shown in Fig. 12. Among all samples, pure (Gd00) sample presented the best J_c–B properties. It was observed that the critical current density decreased considerably with the increase of the amount of Gd. As more grain boundaries have weaker link in the

Gd-added sample, it is thought that the self-field J_c of these samples decreases.

The J_c values of the pure and Gd-added samples at self-field and 8 T magnetic field are given in Table 4. It was seen that the self-field J_c decreased systematically with an

Table 3 Activation energies of the samples (K)

Samples	Activation energy (K)			
	0 T	1 T	3 T	5 T
Gd00	5838	651	395	330
Gd01	435	226	161	133
Gd02	373	205	133	107
Gd03	367	148	100	79
Gd04	314	98	68	60
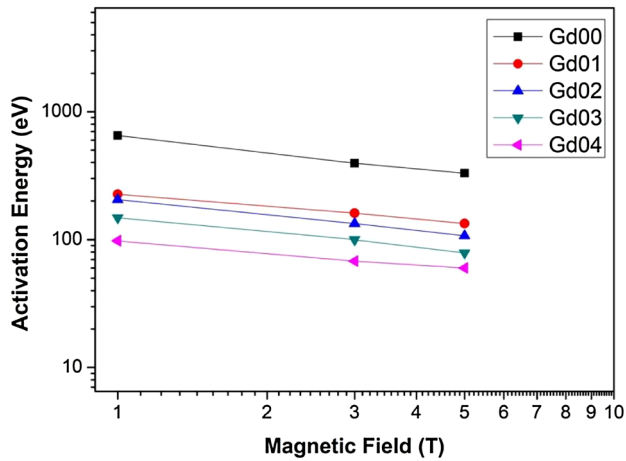
Fig. 10 The magnetic field dependence of the activation energy of the samples

increase in Gd amount. This behaviour can be explained by the superconducting volume deterioration in the samples. From the XRD data, all the samples show the presence of Bi-2223 phase with small amounts of Bi-2212 phase supporting this behaviour.

4 Conclusion

In this study, gadolinium, a rare earth element, was added to BSCCO superconductor, and the effects of this addition on the structural, electrical and magnetic properties of superconductor were investigated in detail. The results obtained in this study are summarized below.

Our investigations have shown that Gd addition weakens the link of the grains and causes to deteriorate the microstructure and superconducting properties of the samples. When the Gd added samples were compared with the pure sample, the following results were obtained:

1) The surface morphology of the microstructure was deteriorated.
2) Conversion to the Bi-2223 phase was prevented.
3) The critical temperature has decreased.
4) Room temperature resistance increased.
5) It was observed that the activation energy (U_0) decreased with the increase in the addition of Gd and applied magnetic field.
6) Gd addition reduced the calculated H_{c2}(T) values.
7) Both J_c and hole number were decreased.

The deterioration of the superconducting properties due to the presence of Gd ions is related to both decreasing percentage of high T_c phase and change of the electronic properties of grain boundaries. It is considered that both the structural and transport properties of the materials deteriorate because of the reduction of the hole concentration by substitution of Ca and Gd ions, and the magnetic characteristics of Gd ions.
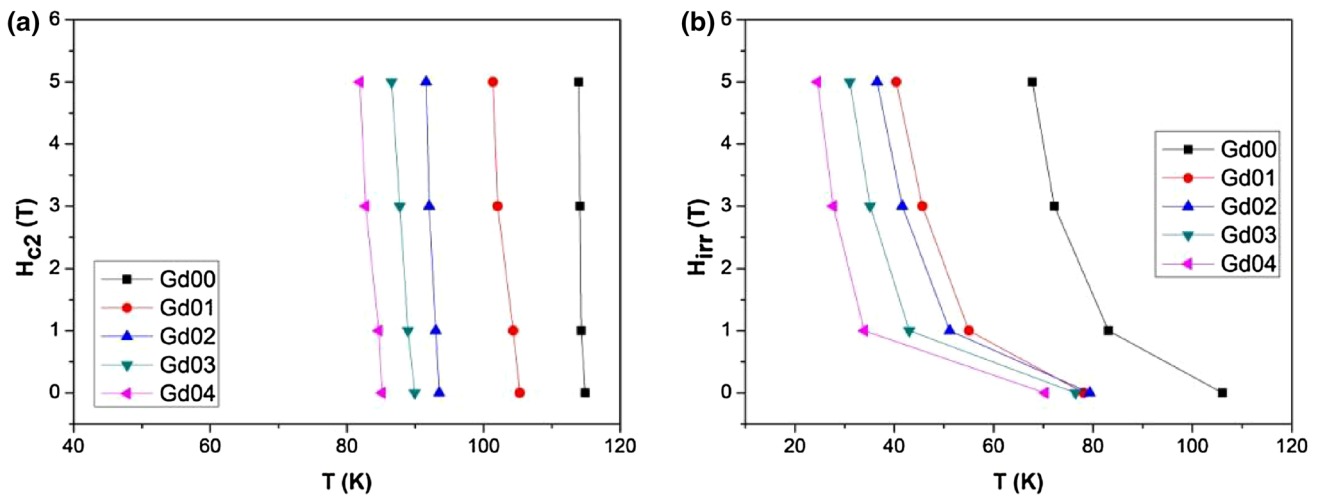
Fig. 11 a The temperature dependence of the upper critical magnetic field (H_{c2}), **b** the temperature dependence of the irreversibility field (H_{irr})
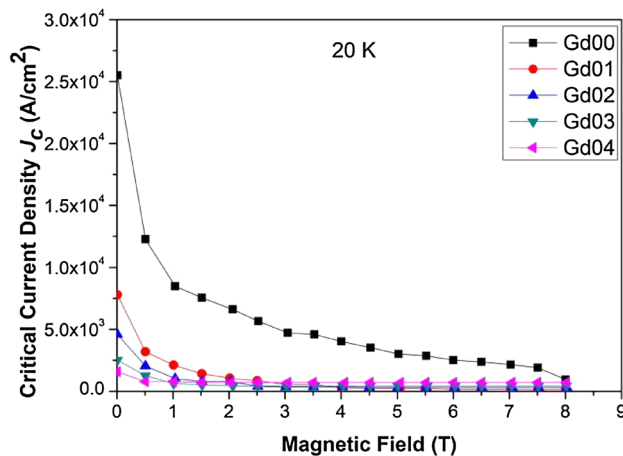
Fig. 12 Critical current densities of all samples at 20 K as a function of applied field

Table 4 The J_c values of the pure and Gd-added samples

Samples	Self field J_c (A/cm^2)	8 T J_c (A/cm^2)
Gd00	2.5×10^4	9.5×10^2
Gd01	7.8×10^3	1.7×10^2
Gd02	4.6×10^3	3.1×10^2
Gd03	2.5×10^3	4.2×10^2
Gd04	1.5×10^3	7×10^2

References

1. M.K. Wu, J.R. Ashburn, C.J. Torng, P.H. Hor, R.L. Meng, L. Gao, Z.J. Huang, Y.Q. Wang, C.W. Chu, Phys. Rev. Lett. **58**, 908–910 (1987)
2. H. Maeda, Y. Tanaka, M. Fukutomi, T. Asano, Jpn. J. Appl. Phys. **27**, 209 (1988)
3. S.A. Sunshine, T. Siegrist, L.F. Schneemeyer, D.W. Murphy, R.J. Cava, B. Batlogg, R.B. Van Dover, R.M. Fleming, S.H. Glarum, S. Nakahara, R. Farrow, J.J. Krajevski, S.M. Zahurak, J.V. Waszczak, J.H. Marshall, P. Marsh, L.W. Rupp, W.F. Peck, Phys. Rev. B **38**, 893 (1988)
4. S.M. Green, C. Jiang, Y. Mei, H.L. Luo, C. Politis, Phys. Rev. B **38**, 5016–5019 (1988)
5. E. Chavira, R. Escudero, D. Rios-Jara, L.M. Leon, Phys. Rev. B **38**, 9272–9275 (1988)
6. N. Hudakova, V. Plechacek, P. Dordor, K. Flachbart, K. Knizek, J. Kovac, M. Reiffers, Supercond. Sci. Technol. **8**, 324–328 (1995)
7. L. Yanrong, B. Yang, J. Mater. Sci. Lett. **13**, 594–596 (1994)
8. M. Muralidhar, D. Mangapathi Rao, T. Somaiah, V. Hari Babu, Cryst. Res. Technol. **561**, 561–565 (2006)
9. M.N. Khan, A. Memon, S. Al-Dallal, M. Al-Othman, M. Zein, W. Alnaser, Mod. Phys. Lett. B **7**, 1687 (1993)
10. W. Alnaser, M. Zein, M.N. Khan, S. AI-Dallal, A. Memon, M.J. AI-Othman, Supercond. Sci. Technol. **6**, 429–436 (1993)
11. M.N. Khan, A.U. Haq, J. Mater. Eng. Perform. **5**, 446–451 (1996)
12. M.N. Khan, A.N. Kayani, A.U. Haq, J. Mater. Sci. **33**, 2365–2369 (1998)
13. M. Daumling, R. Maad, A. Jeremie, R. Flukiger, J. Mater. Res. **12**, 1445–1450 (1997)
14. M. Muralidhar, K. Nanda Kishore, V. Hari Babu, Mater. Chem. Phys. **33**, 117–123 (1993)
15. B. Liang, C. Bernhard, T. Wolf, C.T. Lin, Supercond. Sci. Technol. **17**, 731–738 (2004)
16. J. Yoo, C. Jiang, J. Ko, Y. Kim, H. Kim, H. Chung, Evolution (N. Y). **13**, 3014–3017 (2003)
17. I.H. Gul, M.A. Rehman, M. Ali, A. Maqsood, Phys. C Supercond. Appl. **432**, 71–80 (2005)
18. D. Yegen, C. Terzioglu, Chin. J. Phys. **44**, 233–240 (2006)
19. C. Terzioglu, O. Oztürk, A. Kiliç, A. Gencer, I. Belenli, Phys. C Supercond. Appl. **434**, 153–156 (2006)
20. H. Gündoğmuş, J. Mater. Sci.: Mater. Electron. **28**, 12598–12605 (2017)
21. Y. Himeda, M. Kiuchi, E.S. Otabe, T. Matsushita, J. Fujikami, K. Hayashi, K. Sato, Phys. C. **445–448**, 722–725 (2006)
22. F. Karaboğa, A.T. Ulgen, H. Yetiş, M. Akdoğan, M. Pakdil, I. Belenli, Mater. Sci. Eng. A. **721**, 89–95 (2018)
23. O. Erdem, M. Abdioglu, S.B. Guner, S. Celik, T. Kucukomeroglu, J. Alloys Compds. **727**, 1213–1220 (2017)
24. A.T. Ulgen, J. Baun, Inst. Sci. Technol. **19**, 121–128 (2017)
25. S.B. Guner, S. Celik, A. Cansız, K. Ozturk, J. Supercond. Nov. Magn. **30**, 1335–1343 (2017)
26. C.P. Bean, Rev. Mod. Phys. **36**, 31–39 (1964)
27. M.R. Presland, J.L. Tallon, R.G. Buckley, R.S. Liu, N.E. Flower, Phys. C. **176**, 95–105 (1991)
28. C. Terzioglu, M. Yilmazlar, O. Ozturk, E. Yanmaz, Phys. C. **423**, 119–126 (2005)
29. S. Simon, G. Ilonca, I. Barbur, I. Ardelean, R. Redac, Phys. C Supercond. Appl. **162–164**, 1289–1290 (1989)
30. K. Nanda Kishore, S. Satyavathi, M. Muralidhar, V. Hari Babu, O. Pena, M. Sergent, F. Beniere, Phys. Status Solidi **143**, 101–108 (1994)
31. R.P. Aloysius, P. Guruswamy, U. Syamaprasad, Phys. C Supercond. Appl. **426–431**, 556–562 (2005)
32. J.H. Kim, S.X. Dou, D.Q. Shi, M. Rindfleisch, M. Tomsic, Supercond. Sci. Technol. **20**, 1026–1031 (2007)
33. H. Kitaguchi, A. Matsumoto, H. Hatakeyama, H. Kumakura, Supercond. Sci. Technol. **17**, S486–S489 (2004)
34. A. Coşkun, A. Ekicibil, B. Özçelik, K. Kıymaç, Chin. J. Phys. **21**, 2041–2044 (2004)
35. B. Chevalier, B. Lepine, A. Le Lirzin, J. Darriet, J. Etourneau, Mater. Sci. Eng. B **2**, 277–280 (1989)
36. R.C. Budhani, D.O. Welch, M. Suenaga, R.L. Sabatini, Phys. Rev. Lett. **64**, 1666–1669 (1990)
37. B. Jayaram, P.C. Lanchester, M.T. Weller, Phys. C Supercond. Appl. **160**, 17–24 (1989)
38. C.S. Yadav, P.L. Paulose, New J. Phys. **11**, 0–10 (2009)
39. G.L. Bhalla, A. Pratima, K.K. Malik, Singh, Phys. C Supercond. Appl. **391**, 17–24 (2003)
40. G.B. Smith, J.M. Bell, S.W. Filipczuk, C. Andrikidis, Phys. C Supercond. Appl. **160**, 333–340 (1989)
41. M. Inui, P.B. Littlewood, S.N. Coppersmith, Phys. Rev. Lett. **63**, 2421–2424 (1989)
42. H.K. Liu, Y.C. Guo, S.X. Dou, S.M. Cassidy, L.F. Cohen, G.K. Perkins, A.D. Caplin, N. Savvides, Phys. C Supercond. Appl. **213**, 95–102 (1993)
43. I. Kuševié, E. Babié, Z. Marohnié, J. Ivkov, S.X. Dou, Phys. C Supercond. Appl. **235–240**, 3035–3036 (1994)
44. B. Özkurt, B. Özçelik, J. Low Temp. Phys. **156**, 22–29 (2009)
45. N.V. Vo, H.K. Liu, S.X. Dou, Supercond. Sci. Technol. **9**, 104–112 (1996)
46. M.H. Pu, W.H. Song, B. Zhao, X.C. Wu, Y.P. Sun, J.J. Du, J. Fang, Phys. C Supercond. Appl. **361**, 181–188 (2001)
47. Z.H. Wang, H. Zhang, Phys. C Supercond. Appl. **320**, 218–224 (1999)